EUROPEAN ORGANIZATION FOR NUCLEAR RESEARCH

CERN/EP 87-45
26 February 1987

D-MESON PRODUCTION FROM 400 GeV/c pp INTERACTIONS

LEBC/EHS Collaboration

Aachen[1]-Berlin[2]-Bombay[3]-Brussels[4]-CERN[5]-Collège de France[6]-Duke University[7]-Genova[8]-Japan Universities[9] (Chuo University, Tokyo Metropolitan University, Tokyo Universities of Agriculture and Technology)-Liverpool[10]-Madrid[11]-Mons[12]-Oxford[13]-Padova[14]-Paris[15]-Roma[16]-Rutherford[17]-Rutgers[18]-Serpukhov[19]-Stockholm[20]-Strasbourg[21]-Trieste[22]-Vienna[23]

M. Aguilar-Benitez[11], W.W.M. Allison[13], J.L. Bailly[12], S. Banerjee[3], W. Bartl[23], M. Begalli[1], P. Beillière[6], R. Bizzarri[16], H. Briand[15], R. Brun[5], V. Canale[16], C. Caso[8], E. Castelli[22], P. Checchia[14], P.V. Chliapnikov[19], N. Colino[11], S.J. Colwill[13], R. Contri[8], D. Crennell[17], A. De Angelis[14], L. de Billy[15], C. Defoix[6], R. Di Marco[18], E. Di Capua[16], F. Diez-Hedo[11], J. Dolbeau[6], J. Dumarchez[15], M. Eriksson[20], C. Fernandez[5], C. Fisher[17], Yu.V. Fisyak[19], F. Fontanelli[8], J. Fry[10], S.N. Ganguli[3], U. Gasparini[14], U. Gensch[2], S. Gentile[16], D.B. Gibaut[13], A.T. Goshaw[7], F. Grard[12], A. Gurtu[3], R. Hamatsu[9], L. Haupt[20], S. Hellman[20], J.J. Hernandez[5], S.O. Holmgren[20], M. Houlden[10], J. Hrubec[23], P. Hughes[17], D. Huss[21], Y. Iga[9], M. Iori[16], E. Jegham[21], K.E. Johansson[20], M.I. Josa[11], M. Kalelkar[18], A.G. Kholodenko[19], E.P. Kistenev[19], S. Kitamura[9], D. Knauss[2], V.V. Kniazev[19], W. Kowald[7], D. Kuhn[23], M. Laloum[6], P. Legros[12], H. Leutz[5], M. MacDermott[17], P. Mason[10], M. Mazzucato[14], M.E. Michalon-Mentzer[21], A. Michalon[21], T. Moa[20], R. Monge[8], L. Montanet[5], T. Naumann[2], G. Neuhofer[23], H.K. Nguyen[15], S. Nilsson[20], H. Nowak[2], N. Oshima[9], G. Otter[1], R. Ouared[15], J. Panella Comellas[13], G. Patel[10], M. Pernicka[23], P. Pilette[12], C. Pinori[14], G. Piredda[16], R. Plano[18], A. Poppleton[5], P. Poropat[22], R. Raghavan[3], S. Reucroft[5], K. Roberts[10], W.J. Robertson[7], H. Rohringer[23], J.M. Salicio[11], R. Schulte[1], B. Sellden[20], M. Sessa[22], S. Squarcia[8], P. Stamer[18], V.A. Stopchenko[19], K. Sudhakar[3], K. Takahashi[9], M.C. Touboul[5], U. Trevisan[8], C. Troncon[22], T. Tsurugai[9], E.V. Vlasov[19], C. Voltolini[21], B. Vonck[4], W.D. Walker[7], C.F. Wild[7], T.P. Yiou[15] and G. Zumerle[14]

Submitted to Physics Letters B

---

[1] III. Physikalisches Int. der Technischen Hochschule, Aachen, Germany

[2] Institute für Hochenergiephysik der AdW der DDR, Berlin-Zeuthen, GDR

[3] Tata Institute of Fundamental Research, Bombay, India

[4] IIHE ULB-VUB, Brussels, Belgium

[5] CERN, European Organization for Nuclear Research, Geneva, Switzerland

[6] Lab. de Physique Corpusculaire, Collège de France, Paris, France

[7] Duke University, Durham, NC, USA

[8] Dipartimento di Fisica and INFN, Università di Genova, Genova, Italy

[9] Tokyo University of Agriculture and Technology and Tokyo Metropolitan University, Tokyo, Japan

[10] Phys. Dept. University of Liverpool, Liverpool, UK

[11] CIEMAT-JEN, Madrid, Spain

[12] Université de l'Etat à Mons, Mons, Belgium

[13] Nuclear Physics Laboratory, University of Oxford, Oxford, UK

[14] Dipartimento di Fisica, Università di Padova and INFN, Padova, Italy

[15] LPNHE, Paris 6-Paris 7, Paris, France

[16] Dipartimento di Fisica and INFN, Università of Roma, La Sapienza, Roma, Italy

[17] Rutherford and Appleton Laboratory, Chilton, UK

[18] Rutgers University, New Brunswick, USA

[19] Institute for High Energy Physics, Serpukhov, USSR

[20] Institute of Physics, University of Stockholm, Stockholm, Sweden

[21] Div. High Energy, CRN Strasbourg and Université Louis Pasteur, Strasbourg, France

[22] Dipartimento di Fisica and INFN, Università Trieste, Trieste, Italy

[23] Inst. für Hochenergiephysik der Osterreichischen Akademie der Wissenschaften, Wien, Austria

ABSTRACT

We have measured the inclusive production properties of D and $\bar{D}$ mesons produced from pp interactions at $\sqrt{s} = 27.4$ GeV. The differential production cross section is well represented by the empirical form:

$$d^2\sigma/dx_F dP_T^2 = \frac{\sigma(D/\bar{D})(n + 1)b}{2} (1 - |x_F|)^n e^{-bp_T^2}$$

with $n = 4.9 \pm 0.5$, $b = (1.0 \pm 0.1)(\mathrm{GeV}/c)^{-2}$, and the inclusive $D/\bar{D}$ cross section $\sigma(D/\bar{D})$ is $(30.2 \pm 3.3)\mu b$. The QCD fusion model predicts $D/\bar{D}$ production which is in good agreement with our data except for the magnitude of the cross section which depends sensitively on the assumed mass of the charm quark.

We report here a measurement of D and $\bar{D}$ meson production from pp interactions at 400 GeV/c ($\sqrt{s}$ = 27.4 GeV). The experiment has an unbiased acceptance for charm particles produced with Feynman $x_F > 0$ and can separate $D^{\pm}$ mesons from D_s and Λ_c by means of kinematic fits and good $\pi^{\pm}/K^{\pm}/p^{\pm}$ identification. Our measurement determines the inclusive D/$\bar{D}$ differential production cross section with no model dependent assumptions and therefore provides data which can critically test QCD predictions of charm hadroproduction.

The data were obtained from CERN experiment NA27 which used the Lexan Bubble Chamber (LEBC) and the European Hybrid Spectrometer (EHS) [1]. LEBC served both as a high resolution detector for the charm particle decays and provided a 12 cm long hydrogen target for the 400 GeV/c proton beam. An interaction producing more than two charged particles in a set of downstream PWC's triggered a laser flash. This was delayed 70 μs to allow a bubble diameter of 20 μm which represents the two-track resolution. The bubble density is of the order of 80 cm^{-1}. After measurements on a High Precision Device (HPD) which allows to measure impact parameters with a precision better than 2.5 μm, it was possible to reliably detect tracks from charm decay vertices with impact parameters down to 7 μm. The EHS spectrometer was used to measure the momenta of charged particles to an accuracy of about 0.5% for those particles produced within ~ 120 mrad of the beam direction.

A description of charged particle identification and neutral particle detection in the EHS spectrometer is given elsewhere [1]. We mention here that $\pi^{\pm}/K^{\pm}/p^{\pm}$ separation is accomplished by means of a Silica Aerogel Cerenkov counter, a Helium Cerenkov counter and an ISIS device, while $\gamma/\pi^{o}/\eta^{o}$ and K^{o}_{L}/n detection is made with electromagnetic and neutral hadron calorimeters which cover the forward x_F region.

The charm data sample comes from 1,015,000 pp interactions in the fiducial volume, representing a sensitivity of (38.5 ± 1.1)events/μb. The on-line charged particle multiplicity trigger mentioned above had an efficiency of $(98^{+2}_{-3})\%$ for pp interactions producing charm particles. The data on charm particles are obtained by direct observation of their decays in the bubble chamber. Each frame was double scanned on two views. A "scan box" was defined on the LEBC pictures to reduce the background of strange particles without affecting the charm sample. We refer to ref. [2] for more details on film analysis (see also table 1).

After scanning and measurement we identify 322 pp interactions containing 429 clear charm decays, 52 decays with a charm signature but without a clear topological assignment and 72 decays without a clear charm signature but paired with a charm decay in the same interaction. Our total charm sample consists therefore of 231 interactions with a charm pair and of 91 interactions where only one charm decay is observed. The clear charm decays are distributed into 64 C1, 134 C3, 7 C5, 169 V2, 53 V4 and 2 V6 (Cn for charged, Vn for neutral n-charged decays). The C1 and V2 decays are required to have one decay particle with transverse momentum greater than 250 MeV/c to eliminate strange particle decays which represent the only potential significant background. After this cut, the background is estimated to be less than 1% of the total charm sample of 553 decays. Our charm particle analysis imposes further cuts on these decays to insure good scanning efficiency and, where necessary, good particle acceptance in the EHS spectrometer. The data sample used for the total cross section measurement consists of 217 $D/\bar{D}$ decays while the one used for x_F and p_T^2 differential distributions contains 119 fitted $D/\bar{D}$ decays with $x_F > 0$.

The total cross section was measured using a technique which reduces the systematic error coming from poorly known D meson decay branching ratios. The cross section is given by:

$$\sigma(D) = \frac{\sum_{i=1}^{3} N_i(D)\ w_i(D)/\epsilon_i}{S\ .\ BR}$$

where the summation is over the three observed topologies (C1, C3, C5 for $D^{\pm}$, V2, V4, V6 for D^{o}) and BR the branching ratio for the D decay into the sum of these topological channels [$BR(D^{+}/D^{-} \rightarrow C1 + C3 + C5) = 1.0$ and $BR(D^{o}/\bar{D}^{o} \rightarrow V2 + V4 + V6) = 0.86 \pm 0.04$] [3]. $N_i(D)$ is the number of decays surviving the geometrical cuts shown in table 1. These cuts are applied to guarantee a high detection efficiency and a clean topology definition. In addition, we impose that (n - 1) charged particle decay tracks (and the unique track in the case of C1) fall inside the spectrometer acceptance, i.e. dip $|\lambda|$ and azimuthal angle $|\phi|$ are required to be less than 150 mrad.

$W_i(D)$ is the weight which corrects for events lost due to the cuts and ε_i the scanning plus processing efficiency for each channel varying from 0.85 ± 0.05 for C1's to 0.95 ± 0.05 for decays with more than two charged tracks. S is the experiment sensitivity.

We have verified that the calculated charged D cross section is stable to variations in the impact parameter cuts, showing that any contamination due to D_s and Λ_c decays is small compared to our statistical errors.

The weights, $w_i(D)$, were calculated from a Monte-Carlo generation of D produced with a

$$(1 - |x_F|)^n e^{-bp_T^2}$$

spectrum where the values of n and b were chosen to be consistent with our measured data. They were computed for the dominant decay modes, with the known D meson lifetimes. Repeating the Monte-Carlo simulation with different values of the parameters, we found that the weights are not sensitive to the production properties, i.e. to n and b within $\Delta n = \pm 3$ and $\Delta b = \pm 0.2$. For a variation of 10% in the lifetimes, the weights change by 3% and the uncertainties in the branching ratios also lead to an error of ~ 3%.

Using the above procedure, the inclusive D production cross sections for all x_F are calculated to be:

$$\sigma(D^+/D^-) = (11.9 \pm 1.2)\mu b$$

$$\sigma(D^o/\bar{D}^o) = (18.3 \pm 1.9)\mu b$$

and

$$\sigma(D/\bar{D}) = (30.2 \pm 2.2)\mu b.$$

The errors quoted are statistical. The systematic errors are of the order of 7% for $D^\pm$ and 9% for D^o. They include uncertainties in the weights, in the assignment of unclear topologies and in the contamination which may be due to rare decay modes of strange particles. They also include, for the D^o, the error on the 0-prong branching ratio, and, for the $D^\pm$, the uncertainty due to a possible residual contamination of D_s and Λ_c. Finally, they include the scanning efficiency uncertainty (5%) and the error on the sensitivity of the experiment.

These results can be compared to the cross sections measured in the same experiment for π^- proton interactions at 360 GeV/c [2]:

$$\sigma(D^+/D^-) = (5.7 \pm 1.5)\mu b$$

and

$$\sigma(D^o/\bar{D}^o) = (10.1 \pm 2.2)\mu b$$

at $x_F > 0$. One does not observe significant differences between π^- induced and proton induced D meson total production cross sections.

The analysis making use of D mesons with fully determined momenta is based on 24 D^+, 27 D^-, 29 D^o, 22 $\bar{D}^o$ and 16 $D^o/\bar{D}^o$, 1 $D^\pm$ ambiguous decays at $x_F > 0$. A detailed description of the selection procedure to arrive at such a sample is given in previous publications [2,4].

Using these numbers and the total inclusive cross sections given above, we have estimated the D meson (C = +1) and $\bar{D}$ meson (C = -1) production cross sections.

We find:

$$\sigma(D) = (16.2 \pm 2.0)\mu b$$

and

$$\sigma(\bar{D}) = (14.0 \pm 1.8)\mu b,$$

No significant difference between $\sigma(D)$ and $\sigma(\bar{D})$ is observed. Likewise, no significant difference is observed between $\sigma(D^o)$ and $\sigma(\bar{D}^o)$, or between $\sigma(D^+)$ and $\sigma(D^-)$:

$$\sigma(D^o) = (10.5 \pm 1.7)\mu b$$

$$\sigma(\bar{D}^o) = (7.9 \pm 1.5)\mu b$$

$$\sigma(D^+) = (5.7 \pm 1.0)\mu b$$

$$\sigma(D^-) = (6.2 \pm 1.0)\mu b$$

Using the sample of 231 charm-anticharm pairs we have also evaluated the following $D\bar{D}$ pair cross sections:

$$\sigma(D^+D^-) = (2.5 \pm 0.6)\mu b$$

$$\sigma(D^+\bar{D}^o + c.c.) = (6.2 \pm 1.1)\mu b$$

$$\sigma(D^o\bar{D}^o) = (5.9 \pm 1.3)\mu b$$

yielding a total $D\bar{D}$ pair cross section of

$$\sigma(D\bar{D}) = (14.6 \pm 1.8)\mu b.$$

Having obtained a sample of D with measured momenta, we can search for $D^*(2010)$ mesons by making use of the decay channel $D^* \to D\pi$. An analysis of the $D\pi$ mass spectra shows background-subtracted signals of $(23 \pm 5)D^{*+}/D^{*-} \to D^o/\bar{D}^o\pi^\pm$ and $(8 \pm 3.5)D^{*o}/\bar{D}^{*o} \to D^o/\bar{D}^o\pi^o$ decays. For D^* with $x_F > 0$ the efficiency for the reconstruction of the decay pion, ε_π, is 0.95 ± 0.05 (0.50 ± 0.07) for the $\pi^\pm(\pi^o)$. The D^* production cross sections are determined from these data and the branching ratios $BR(D^{*+} \to D^o\pi^+) = 0.49 \pm 0.08$ and $BR(D^{*o} \to D^o\pi^o) = 0.52 \pm 0.08$ [5]:

$$\sigma(D^*) = \frac{N(D^* \to D\pi)}{\varepsilon_\pi \, BR(D^* \to D\pi)} \cdot \frac{\sigma(D^o/\bar{D}^o)}{N(D^o/\bar{D}^o)}$$

Using the sample of 98 $D^o/\bar{D}^o$decays (for the analysis of the D^* signal we do not have to restrict the D^o, $\bar{D}^o$ sample to the D meson with fully determined momentum), and our measured $D^o/\bar{D}^o$ production cross section of $(18.3 \pm 1.9)\mu b$, the inclusive D^* production cross sections (all x_F) are calculated to be

$$\sigma(D^{*+}/D^{*-}) = (9.2 \pm 2.2)\mu b$$

$$\sigma(D^{*o}/\bar{D}^{*o}) = (5.8 \pm 2.6)\mu b$$

and

$$\sigma(D^*/\bar{D}^*) = (15.0 \pm 3.4)\mu b$$

These cross sections when compared to the total D production cross sections, show that the $D^*(2010)$ is an important source of the observed D mesons: $\sigma(D^\pm$ from $D^*)/\sigma(D^\pm) = 0.39 \pm 0.11$ and $\sigma(D^o$ from $D^*)/\sigma(D^o) = 0.56 \pm 0.17$. More specifically, if the ratio of direct D^* to direct D production is given by r, then

$$\sigma(D^*/\bar{D}^*)/\sigma(D/\bar{D}) = r/(1 + r).$$

A simple counting of available helicity states predicts $r = 3$ and $\sigma(D^*/\bar{D}^*) = 3/4\ \sigma(D/\bar{D}) = (23 \pm 2)\mu b$. This is to be compared with our measurement of $(15.0 \pm 3.4)\mu b$.

With incident π^- at 360 GeV/c, we found a total D^* cross section in the forward hemisphere of $(12.3 \pm 3.6)\mu b$ [6], slightly larger than the value reported here for incident protons.

The measured $d\sigma/dx_F$ and $d\sigma/dp_T^2$ spectra for the $D/\bar{D}$ mesons are shown in fig. 1. The data have been corrected for the bubble chamber visibility and spectrometer acceptance efficiencies. The solid curves in fig. 1 show the result of a fit of the D production spectrum to the simple empirical form:

$$d^2\sigma/dx_F dp_T^2 \propto (1 - x_F)^n e^{-bp_T^2} \quad .$$

This reproduces the measured spectrum well with $n = 4.9 \pm 0.5$ and $b = (1.0 \pm 0.1)(\mathrm{GeV}/c)^{-2}$. The average transverse momentum of the D $\langle p_T \rangle = (0.86 \pm 0.09)\mathrm{GeV}/c$, is similar to that observed in most other charm hadroproduction reactions [7]. The x_F spectrum is central with $\langle x_F \rangle = 0.15 \pm 0.02$. We emphasize that our experiment is sensitive to D's produced with all $x_F > 0$ and that the data show that the production of leading D is small

$$\frac{\sigma(D/\bar{D})\ x_F > 0.5}{\sigma(D/\bar{D})\ x_F > 0.0} = 0.02^{+0.02}_{-0.01} \quad .$$

We note that the D^- and D^o follow the average x_F, p_T distributions, whereas the D^+ have the hardest distribution ($n = 3.1 \pm 0.8$, $b = 0.8 \pm 0.1$) and the $\bar{D}^o$ the softest ($n = 8.1 \pm 1.9$, $b = 1.5 \pm 0.3$). In contrast to the π^- data, where a leading valence quark effect was observed [4], we see no significant difference between D and $\bar{D}$ (only the $\bar{D}$ could contain a proton valence quark). No correlation was observed between n and lifetime, giving further evidence against a Λ_c contamination of the $D^\pm$ sample.

The QCD fusion model can be used to calculate the D meson production spectrum. The calculation requires: (a) a description of the parton content of the proton, (b) a calculation of the cross sections for the subprocesses $gg \to c\bar{c}$ and $q\bar{q} \to c\bar{c}$ and (c) some approximation to the $c \to D$ fragmentation process. Since the predictions of the model depend on the detailed treatment of the above components, we have allowed some range of input ingredients. For a description of the parton content of the proton we use structure functions determined by Duke and Owens and Eichten et al. (EHLQ) [8]. The intrinsic parton transverse momentum, k_T, is described by the distribution

$$\frac{dN}{dk_T^2} = \frac{1}{\langle k_T^2 \rangle} e^{-k_T^2/\langle k_T^2 \rangle}$$

with $\langle k_T^2 \rangle$ allowed to vary between zero and $0.64(\mathrm{GeV}/c)^2$ [9]. The subprocess cross sections are given by Combridge [10]. For the $c\bar{c}$ production threshold we use $(2\ m_c)^2$ where the charm quark mass is allowed to vary between 1.2 and 1.4 GeV/c^2. The strong interaction coupling constant is given by $\alpha_s = (12\ \pi/25)/\log(Q^2/\Lambda^2)$ where Λ is taken to be 0.2 GeV and Q^2 is allowed to vary between $(2\ m_c)^2$ and s of the parton subprocess. Finally, we have investigated the sensitivity of the D meson differential production cross section to two different $c \to D$ fragmentation processes: a δ-function in which the entire momentum of the c quark is transferred to the D meson and a fragmentation which approximates the final state $c\bar{q}$ and $\bar{c}q$ recombination via colour string breaking as described by the Lund model [11]. The latter depends on adjustable string parameters but these were not changed from the values determined by the Lund group from other data.

Comparisons of some predictions of this QCD fusion model, normalized to our data, are shown in fig. 2. The calculated x_F and p_T^2 distributions are relatively insensitive to the choice of structure function and charm quark mass. The curves presented in fig. 2 were obtained using EHLQ set one structure functions and a charm quark mass of 1.25 GeV/c^2. The $d\sigma/dp_T^2$ distribution is sensitive to the parton intrinsic k_T and when given the choice of zero or $\langle k_T^2 \rangle = 0.64(\mathrm{GeV}/c)^2$ (the value determined from Drell-Yan measurements) our data select $0.64(\mathrm{GeV}/c)^2$.

The dashed curve in fig. 2(a) shows the fusion model predictions with inputs fixed as described in the above paragraph and using a δ-function

$c \rightarrow D$ fragmentation. This illustrates the basic parton-level prediction. The Lund fragmentation scheme results in a somewhat broader D meson x_F spectrum in the central region. This prediction is given by the solid curves in fig. 2 and agrees with all features of the measured $D/\bar{D}$ x_F and p_T distributions.

A comparison of the $D/\bar{D}$ inclusive cross section, $\sigma(D/\bar{D})$, to a QCD prediction is less conclusive. In order to calculate $pp \rightarrow D/\bar{D}\ X$, an estimate of the fraction of $c(\bar{c})$ quarks producing $D(\bar{D})$ mesons must be made. Using the Lund fragmentation scheme as a guide, the fraction $\sigma(pp \rightarrow D/\bar{D}\ X)/\sigma(pp \rightarrow c/\bar{c}\ X)$ is found to be 0.7.

Using the EHLQ set one structure functions and $\hat{s}$ (threshold) $= Q^2 = (2\ m_c^2)$, we find for the ratio between our measured $D/\bar{D}$ inclusive cross section and the fusion model prediction

$$k = \frac{\sigma(pp \rightarrow D/\bar{D}\ X)}{0.7\ \sigma(pp \rightarrow c/\bar{c}\ X)} = 1.2 \text{ to } 2.7$$

where the range corresponds to changing m_c from 1.2 to 1.4 GeV/c^2. Based upon the known limitations of the fusion model calculation, the magnitude of this charm k-factor is not surprising.

In summary, we have made a model independent measurement of D and $\bar{D}$ meson production from pp interaction at $\sqrt{s} = 27.4$ GeV. Our measured value of $\sigma(D/\bar{D})$ is $(30.2 \pm 3.3)\mu b$, where the statistical and systematic errors have been added in quadrature. It is larger than the fusion model predictions by a factor of about two, but the theoretical calculations are subject to appreciable uncertainties. No significant difference between $\sigma(D)$ and $\sigma(\bar{D})$ is observed. The measured value of $D\bar{D}$ pair production cross section is $(14.6 \pm 1.8)\mu b$. The inclusive production cross section of $D^*(2010)$ is $\sigma(D^*/\bar{D}^*)$ is $(15.0 \pm 3.4)\mu b$. The global $D/\bar{D}$ production is central with $d\sigma/dx_F \propto (1 - |x_F|)^{4.9\pm0.5}$, although significant differences are observed for D^+ and $\bar{D}^0$ mesons. A fusion model calculation predicts the correct shape of both the x_F and p_T spectra.

We would like to acknowledge the specialists of the bubble chamber and of the SPS, the painstaking work of the scanning staff at the collaborating laboratories and the organization and typing work of our secretaries. Finally, we would like to thank the various funding agencies of our collaboration for making this work possible.

REFERENCES

[1] M. Aguilar-Benitez et al., The EHS spectrometer, submitted to Nucl. Instr. & Meth., January 1987.

[2] M. Aguilar-Benitez et al., Z. Phys. C31 (1986) 491.

[3] M. Aguilar-Benitez et al., Phys. Lett. 135B (1984) 237.

[4] M. Aguilar-Benitez et al., Phys. Lett. 161B (1985) 400.

[5] Review of Particle Properties, Phys. Lett. 170B (1986) 27.

[6] M. Aguilar-Benitez et al., Phys. Lett. 169B (1986) 106.

[7] S. Reucroft, Charm Hadroproduction, XXI Rencontre de Moriond, Les Arcs (1986), vol. 2, p. 323 (ed. by J. Tran Thank Van, Ed. Frontières).

[8] D.W. Duke and J.F. Owens, Phys. Rev. D30 (1984) 49.

E. Eichten et al., Rev. Mod. Phys. 56 (1984) 667.

[9] B. Cox and P.K. Malhotra, Phys. Rev. D29 (1984) 63.

[10] B.L. Combridge, Nucl. Phys. B151 (1979) 429.

[11] H.U. Bengtsson, CHARIS - The Lund Monte-Carlo for charm production (private communication);

H.U. Bengtsson and G. Ingelman, Comp. Phys. Comm. 34 (1985) 231.

TABLE

Geometrical cuts applied to select the charm decays used for the D/$\bar{D}$ total cross section calculations

Decay channel	Decays surviving all cuts N_i (D)	Decay length		Transverse length (mm)	Minimum impact parameter Lower limit (µm)	Maximum impact parameter range (µm)
		Lower	Upper limit (mm)			
C1	39	2	90	0.6		100 to 1500
C3	74	1		2.0	20	100 to 2000
C5	6	1		2.0	20	100 to 2000
V2	67	2	30	0.2	20	60 to 500
V4	30	1		2.0	20	60 to 1500
V6	1	1		2.0	20	60 to 1500

FIGURE CAPTIONS

Fig. 1 (a) $d\sigma/dx_F$ and (b) $d\sigma/dp_T^2$ distribution for $D/\bar{D}$ meson production from pp interactions at $\sqrt{s} = 27.4$ GeV. The solid curves are fits to the data using distributions of the form $(1 - x_F)^n e^{-bp_T^2}$. The fits determine $n = 4.9 \pm 0.6$ and $b = (1.0 \pm 0.1)(\mathrm{GeV}/c)^{-2}$.

Fig. 2 Comparisons of the measured inclusive $D/\bar{D}$ $d\sigma/dx_F$ and $d\sigma/dp_T^2$ distributions to the fusion model calculation described in the text. The dashed curve shows the basic parton level prediction (δ-function $c \rightarrow D$ fragmentation) and the solid curve includes fragmentation effects as simulated by coloured string breaking (the Lund model).

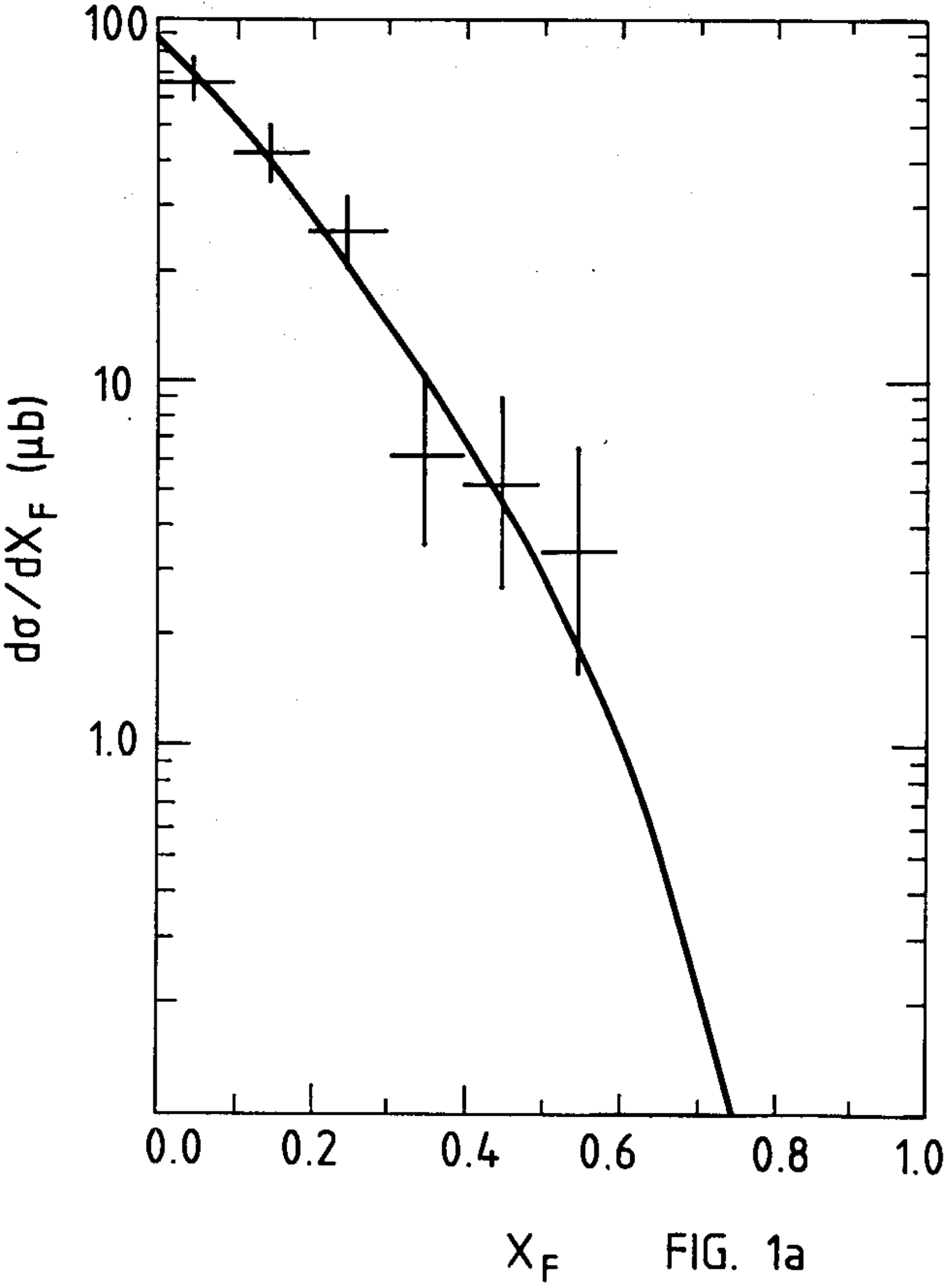

FIG. 1a

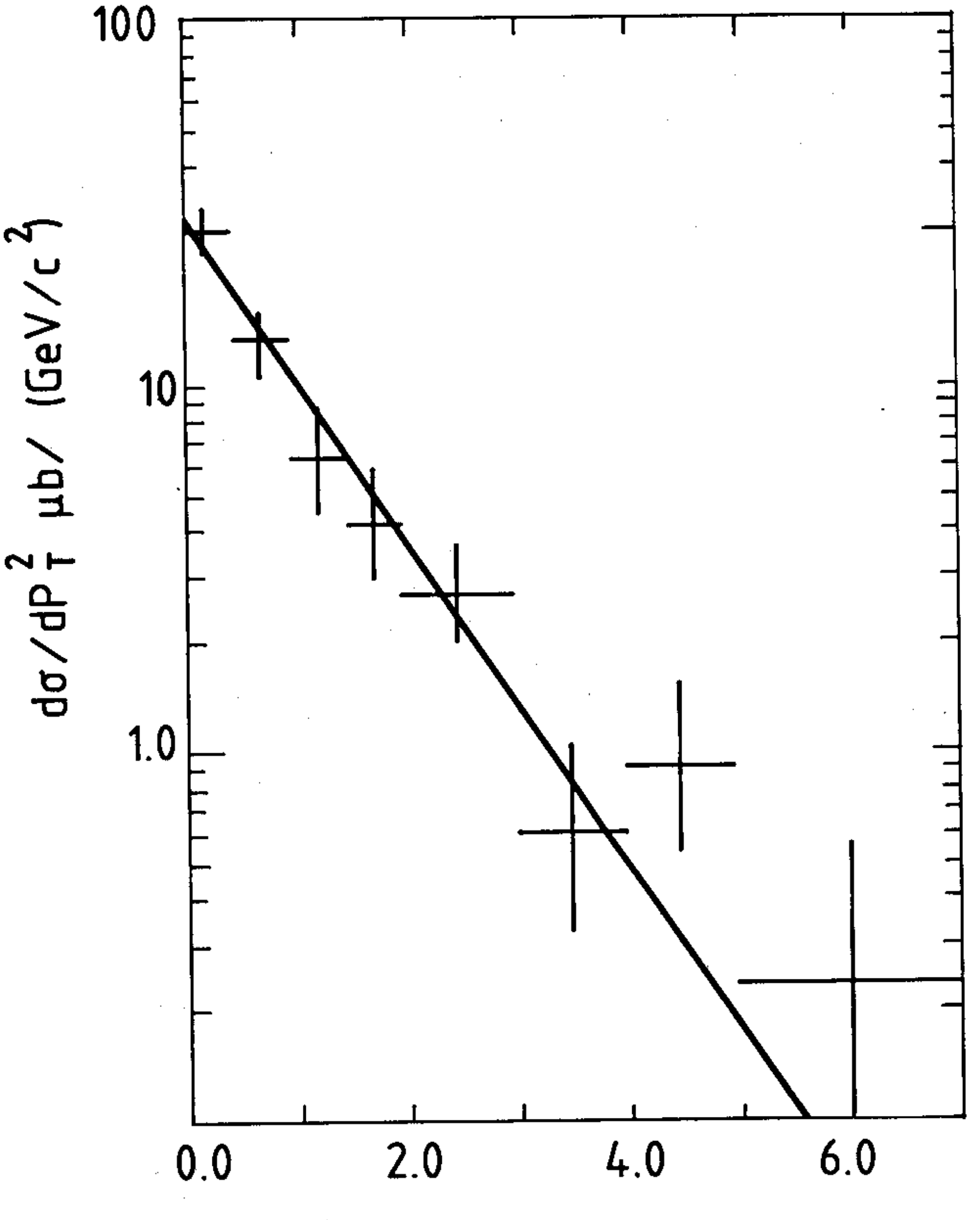

FIG. 1b

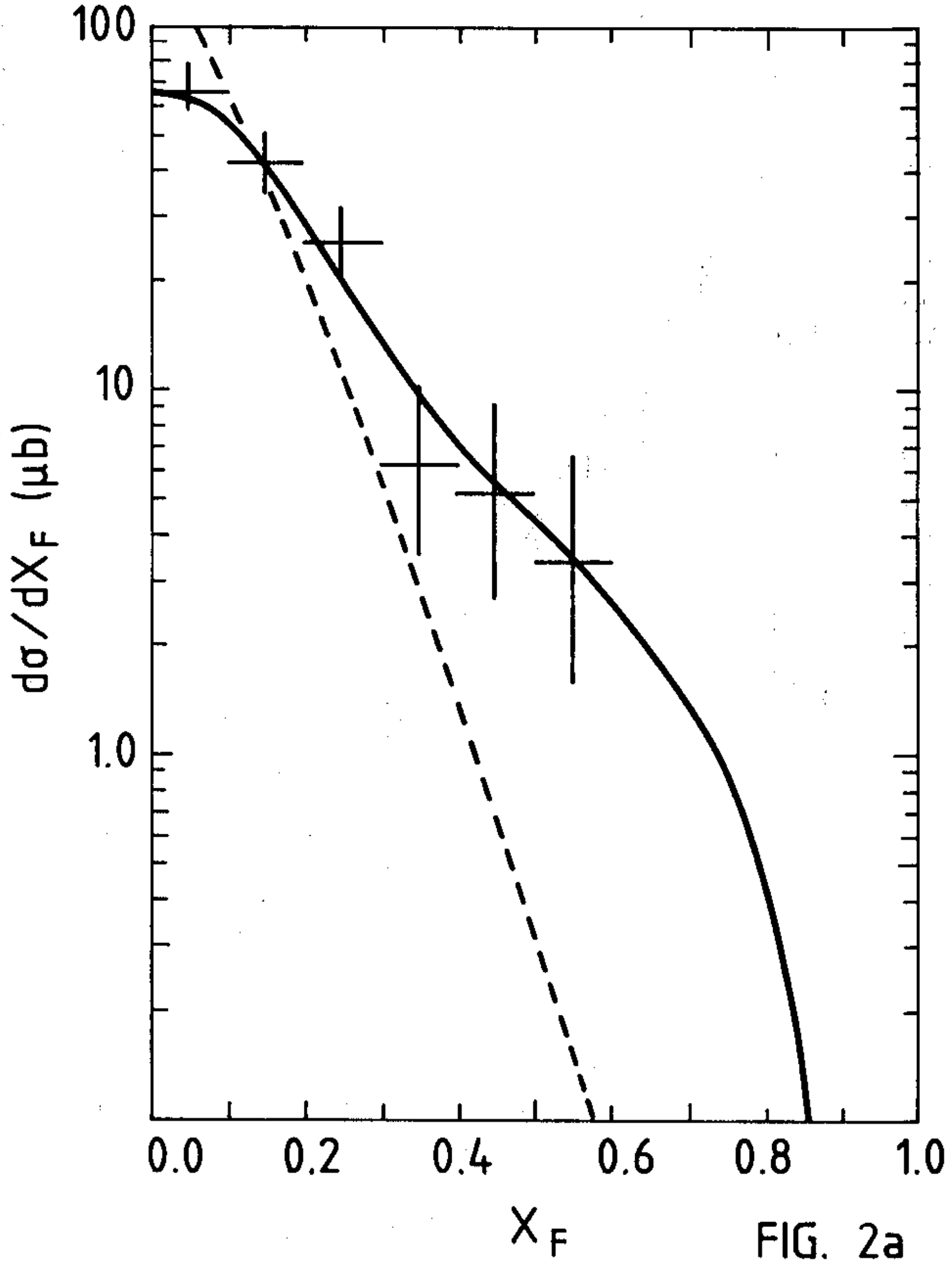

FIG. 2a

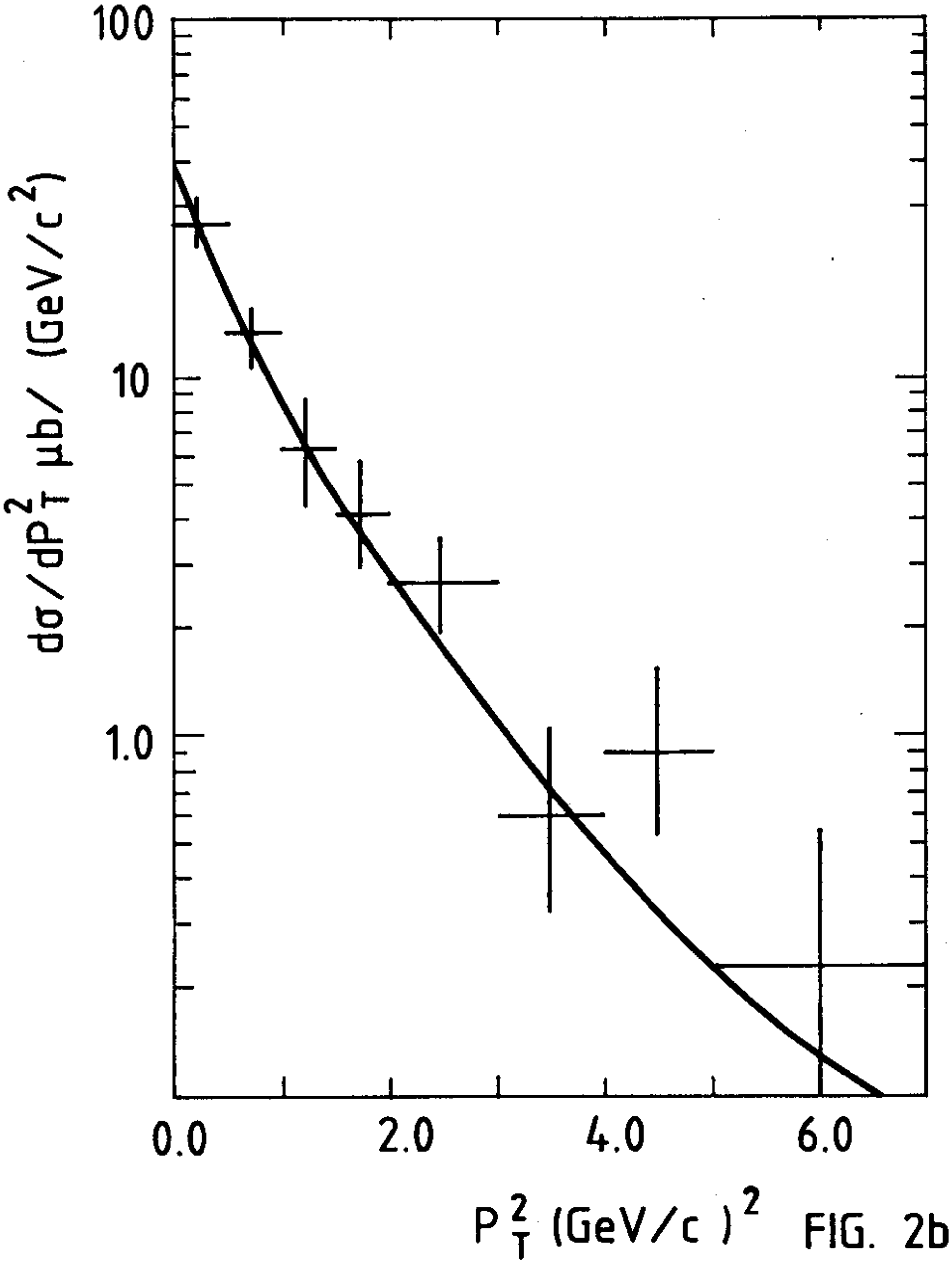

FIG. 2b